



## A new bisepoxyignan dendranlignan A isolated from Chrysanthemum Flower inhibits the production of inflammatory mediators via the TLR4 pathway in LPS-induced H9c2 cardiomyocytes

Mengnan Zeng<sup>a,b,1</sup>, Meng Li<sup>a,b,1</sup>, Yingjie Chen<sup>c</sup>, Jingke Zhang<sup>a,b</sup>, Yangang Cao<sup>a,b</sup>, Beibei Zhang<sup>a,b</sup>, Weisheng Feng<sup>a,b</sup>, Xiaoke Zheng<sup>a,b,\*</sup>, Zhiling Yu<sup>c,\*\*</sup>

<sup>a</sup> Henan University of Chinese Medicine, Zhengzhou, 450046, China

<sup>b</sup> The Engineering and Technology Center for Chinese Medicine Development of Henan Province, Zhengzhou, 450046, China

<sup>c</sup> Centre for Cancer and Inflammation Research, School of Chinese Medicine, Hong Kong Baptist University, Kowloon Tong, Hong Kong

### ARTICLE INFO

#### Keywords:

Dendranlignan A  
Bisepoxyignan  
Structural elucidation  
TLR4  
Cardiomyocyte

### ABSTRACT

A new bisepoxyignan dendranlignan A (A1) and the known compound lantibeside D (D2) was isolated from Chrysanthemum Flower, the dried capitulum of *Dendranthema morifolium* (Ramat.) kitam. Their structures were determined on the basis of extensive spectroscopic methods, including 1D-NMR, 2D-NMR and MS data. Additionally, A1 and D2 were evaluated for their effects on the production of inflammatory mediators in H9c2 cardiomyocytes stimulated with lipopolysaccharide (LPS). Results demonstrated that A1 and D2 decreased LPS-induced production of inflammatory cytokines TNF- $\alpha$ , IL-2 and IFN- $\gamma$  in H9c2 cells. Both compounds also decreased the nuclear localization of c-JUN, p-P65 and p-IRF3, but did not affect the level of TLR4. Molecular docking indicated that A1 and D2 occupied the ligand binding sites of TLR4-MD2. In the present study, we for the first time discovered a new bisepoxyignan compound A1, and found that this compound has a potential to inhibit inflammation by inhibiting TLR4 signaling.

### 1. Introduction

Sepsis is a systemic inflammatory reactive disease. Its progress is rapid and life-threatening, thereby contributing largely to the high sepsis mortality [1]. Recent studies have shown that heart failure is a common complication of sepsis [2,3]. Myocardial dysfunction caused by sepsis is also the main cause of death in patients with sepsis [4]. However, the causes of myocardial dysfunction caused by sepsis have not yet received much attention. It was found that the proinflammatory factors produced by cardiomyocytes, as well as the apoptosis of cardiomyocytes play a key role in the pathogenesis of the myocardial dysfunction [5,6]. Lipopolysaccharide (LPS) has been widely applied to induce apoptosis and myocardial cells [7]. Therefore, the application of LPS-induced apoptosis of the cardiomyocytes could be an effective model for studying myocardial dysfunction caused by sepsis.

*Dendranthema morifolium* (Ramat.) (Flos chrysanthemum) is one of the well-known daily beverage in China, and is known to exhibit antibacterial [8], antioxidant [9], anti-inflammatory, and cardioprotective

characteristics [10]. Flos chrysanthemum is recorded in the Shen Nong's herbal classic and mainly contains flavonoids, triterpenoids, glycosides, and alkaloids [11,12]. Huai Flos Chrysanthemi, one of four major Huai medicines, also one of Flos chrysanthemum, is mainly produced in Jiaozuo of Henan province [13]. In our previous study, four new sesquiterpenoids *viz.* chrysanthguaianolactones and four known sesquiterpenoids were isolated from the acetone extract of Huai Flos chrysanthemum, and the anti-inflammatory activity was investigated using the LPS induced H9c2 cardiomyocytes [14,15]. Since, cardiomyocyte injury is the leading cause of morbidity and mortality in cardiomyopathy patients, such as sepsis [16], diabetes [17], and hypertension [18], the search for effective drugs to protect the cardiomyocyte injury will ultimately cure many diseases.

In continuation of our study on the Huai Flos chrysanthemum, further phytochemical studies were undertaken, which led to the isolation of a new bisepoxyignan Dendranlignan A (A1) and a known compound lantibeside D (D2). The structures of the isolated compounds were confirmed on the basis of spectroscopic analysis, including

\* Corresponding author. Henan University of Chinese Medicine, Zhengzhou, 450046, China.

\*\* Corresponding author.

E-mail addresses: [zhengxk.2006@163.com](mailto:zhengxk.2006@163.com) (X. Zheng), [zlyu@hkbu.edu.hk](mailto:zlyu@hkbu.edu.hk) (Z. Yu).

<sup>1</sup> These authors contributed equally to this work.

UV, IR, 1D and 2D NMR, and HR-ESI-MS. The absolute configurations of A1 and D2 were established by the comparison of the experimental and calculated electronic circular dichroism (ECD) spectra. In addition, we also investigated the protective effects of A1 and D2 from *Huai Flos chrysanthemum* on the LPS-induced injury in H9c2 cardiomyocytes, in order to evaluate its effectiveness to protect the cardiomyocyte injury.

## 2. Materials and methods

### 2.1. General experimental procedures

NMR spectra (including 1D and 2D) were recorded at room temperature (approximately 20–25 °C) on a Bruker Avance III 500 MHz spectrometer using TMS as a standard (500 MHz for <sup>1</sup>H NMR and 125 MHz for <sup>13</sup>C NMR). ECD spectra were obtained on a Chirascan CD spectrometer (Applied Photophysics) at room temperature. Optical rotation was analyzed using the APIV (Rudolph Research Analytical). IR spectrometry was performed using Nicolet iS10 Microscope Spectrometer (Thermo Fisher Scientific). HR-ESI-MS spectra were obtained on a Brukerma Xis HD mass spectrometer. UV spectra were obtained on a Shimadzu UV-2401PC apparatus. Preparative HPLC was conducted using a Saipuruishi LC-50 instrument with a UV200 detector and YMC-Pack ODS-A column (250 × 20 mm, 5 μm and 250 × 10 mm, 5 μm). Column chromatography was performed using a Diaion HP-20 (Mitsubishi Chemical Corporation), Toyopearl HW-40, MCI gel CHP-20 (TOSOH Corporation), Sephadex LH-20 (Amersham Pharmacia Biotech AB), LiChroprep RP-18 gel (Merck, Darmstadt) and silica gel (Marine Chemical Industry). TLC was performed using self-made silica gel G plates (Qingdao Marine Chemical Industry). All chemical reagents were supplied by Beijing Chemical Plant, China and Tianjin NO. 3 Reagent Plant, China.

### 2.2. Plant materials

*Dendranthema morifolium* (Ramat.) S. Kitam was collected from the Jiaozuo, Henan Province, China, in 2015, and identified by Prof. Suiqing Chen (Henan University of Chinese Medicine). A voucher specimen (No. 20150715A) was deposited in the Research Department of Natural Medicinal Chemistry, School of Pharmacy, Henan University of Chinese Medicine.

### 2.3. Extraction and isolation

The plant *Chrysanthemum morifolium* Ramat (11.2 Kg) was extracted using 50% acetone (25 L × 3) thrice in a flash extractor at room temperature (25 °C). The filtered solution was concentrated under reduced pressure to give an extract (2.5 kg). The extract was concentrated further, under reduced pressure to give brown syrup, which was added with water (9 L) and extracted successively by partitioning with petroleum ether (5 × 3 L), EtOAc (5 × 104 L), and n-BuOH (5 × 4 L); the extracts were kept separately. The EtOAc-soluble fraction (352.0 g) was passed through a silica gel (1.0 Kg) open column (30 cm × 16 cm i.d.) eluted with CH<sub>2</sub>Cl<sub>2</sub>/MeOH (v/v, 50:1, 30L → 30:1, 30L → 20:1, 30L → 5:1, 30L) to provide fractions A–D on the basis of TLC analysis. Fraction C (31.0 g) was separated on silica gel CC again, eluting with CH<sub>2</sub>Cl<sub>2</sub>-MeOH (80:1, 60:1, 40:1, 20:1, 10:1, and 5:1), to obtain fractions C1–C6. Fraction C4 was separated by MCI using gradient elution (100% H<sub>2</sub>O to 40% MeOH) to give seven fractions (Fr.C4a – Fr.C4g) based on TLC analysis. Fr.C4f was subjected to Sephadex LH-20 CC by eluting with MeOH: H<sub>2</sub>O (70:30) to afford Fr.C4f1 and Fr.C4f2. Fr.C4f2 was further purified by RP-C18 HPLC [YMC-Pack ODS-AA, CH<sub>3</sub>CN-H<sub>2</sub>O (23:77, v/v) containing 0.2% TFA] to afford compound 1 (t<sub>R</sub> 62.0 min, 2.19 mg) and 2 (t<sub>R</sub> 57.3 min, 2.80 mg).

**Table 1**

NMR spectral data of compounds 1 (A1) and 2 (D2).

| No.                  | $\delta_{\text{H}}$      |                          | $\delta_{\text{C}}$ |       |
|----------------------|--------------------------|--------------------------|---------------------|-------|
|                      | A1                       | D2                       | A1                  | D2    |
| 1                    |                          |                          | 135.6               | 136.8 |
| 2                    | 6.70 (1H, s)             | 6.87 (1H, d, 2.0)        | 104.8               | 107.5 |
| 3                    |                          |                          | 154.4               | 149.4 |
| 4                    |                          |                          | 139.5               | 148.6 |
| 5                    |                          | 6.77 (1H, d, 8.0)        | 154.4               | 109.0 |
| 6                    | 6.70 (1H, s)             | 6.83 (1H, dd, 2.0, 8.0)  | 104.8               | 120.6 |
| 7                    | 4.70 (1H, d, 5.0)        | 4.70 (1H, d, 5.0)        | 87.3                | 87.0  |
| 8                    | 3.10 (1H, m)             | 3.10 (1H, m)             | 55.7                | 55.5  |
| 9                    | 4.25 (1H, m)             | 4.23 (1H, m)             | 72.9                | 72.7  |
|                      | 3.86 (1H, m)             | 3.86 (1H, m)             |                     |       |
| 1'                   |                          |                          | 136.5               | 137.7 |
| 2'                   | 6.87 (1H, d, 2.0)        | 7.01 (1H, d, 2.0)        | 107.5               | 111.6 |
| 3'                   |                          |                          | 149.4               | 150.1 |
| 4'                   |                          |                          | 148.6               | 147.7 |
| 5'                   | 6.77 (1H, d, 8.0)        | 7.13 (1H, d, 8.0)        | 109.0               | 118.1 |
| 6'                   | 6.84 (1H, dd, 2.0, 8.0)  | 6.90 (1H, dd, 2.0, 8.0)  | 120.6               | 119.8 |
| 7'                   | 4.75 (1H, d, 5.0)        | 4.74 (1H, d, 5.0)        | 87.2                | 87.3  |
| 8'                   | 3.10 (1H, m)             | 3.10 (1H, m)             | 55.5                | 55.6  |
| 9'                   | 4.25 (1H, m)             | 4.23 (1H, m)             | 72.8                | 72.7  |
|                      | 3.86 (1H, m)             | 3.86 (1H, m)             |                     |       |
| 1''                  | 4.80 (1H, d, 8.0)        | 4.87 (1H, d, 7.0)        | 105.3               | 102.8 |
| 2''                  | 3.46 (1H, m)             | 3.47 (1H, m)             | 75.7                | 74.9  |
| 3''                  | 3.40 (1H, m)             | 3.38 (1H, m)             | 78.3                | 78.2  |
| 4''                  | 3.40 (1H, m)             | 3.38 (1H, m)             | 71.3                | 71.3  |
| 5''                  | 3.18 (1H, m)             | 3.38 (1H, m)             | 77.8                | 77.8  |
| 6''                  | 3.80 (1H, dd, 2.0, 12.0) | 3.80 (1H, dd, 2.0, 12.0) | 62.6                | 62.6  |
|                      | 3.65 (1H, dd, 7.0, 12.0) | 3.65 (1H, dd, 7.0, 12.0) |                     |       |
| 2 × OCH <sub>3</sub> | 3.85 (6H, s)             | 3.86 (3H, s)             | 57.1                | 55.5  |
| -OCH <sub>2</sub> -  | 5.92 (2H, s)             | 5.92 (2H, s)             | 102.4               | 102.4 |

### 2.4. Acid hydrolysis

Compound 1 (1 mg) was treated with 2 mol/L aqueous HCl (2 mL) (sealed flask, heating in water bath, 80 °C, 3 h). Then the acidic aqueous mixture was dried, water (2 mL) was added, and the mixture was extracted with EtOAc (3 × 2 mL). The aqueous layer was subjected to the chiral-phase HPLC analysis under the following conditions: The carbohydrate products of the hydrolysis of 1 was separated and detected using a CHIRALPAK AD-H column (250 × 4.6 mm) using n-hexane: EtOH: TFA (750:250:0.25) as the mobile phase (0.5 mL min<sup>-1</sup>) using an evaporative light scattering detector (ELSD). D-Glucose was detected in the acid hydrolysates of compound 1 by comparing the retention times of their derivatives with those of known D-glucose derivatives (t<sub>R</sub>, 18.3 min) prepared in the same manner. Glucose samples for comparison were procured from Shanghai Yuanye Biotechnology Co., Ltd., China.

### 2.5. Cell culture and treatment

The H9c2 cardiomyocytes were obtained from the American Type Culture Collection (Manassas, VA, USA). The cells were cultured in DMEM at 37 °C under a humidified atmosphere of 5% CO<sub>2</sub> in air. Heat inactivated FBS (10%) and antibiotics penicillin/streptomycin (1%) were included in the culture. H9c2 cells were seeded on 96-well plates (5000 cells/well, 100 μL) and allowed to adhere overnight. Then, the cells were divided into the control group, model group (LPS 20 μg/mL, Sigma, USA), compound 1 group (10 μM, LPS 20 μg/mL) and compound 2 group (10 μM, LPS 20 μg/mL). Twenty-four hours later, the cell morphology was observed and the cell vitality was detected by the MTT assay (Amresco, Seattle, United States). Real Time Cellular Analysis (RTCA, Acea Biosciences, Inc.) was used to calculate EC<sub>50</sub> of A1 and D2 [19].

### 2.6. Cytometric bead array (CBA) assay

The cell processing was performed in a similar manner as mentioned

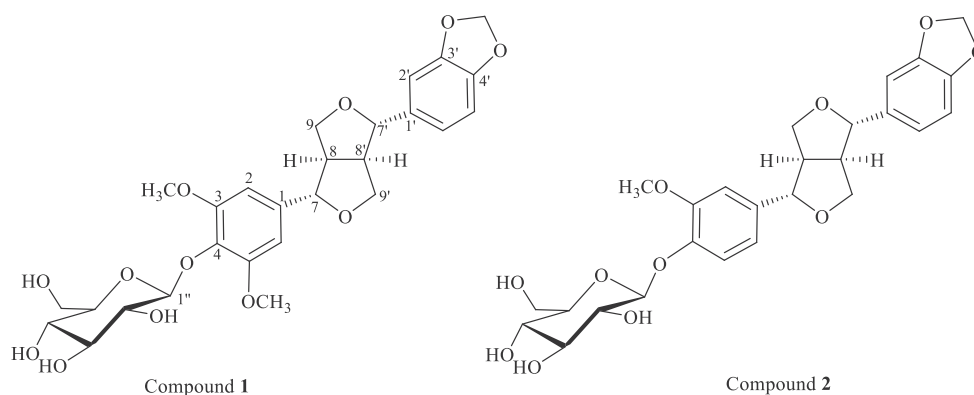


Fig. 1. Structures of compounds 1 (A1) and 2 (D2).

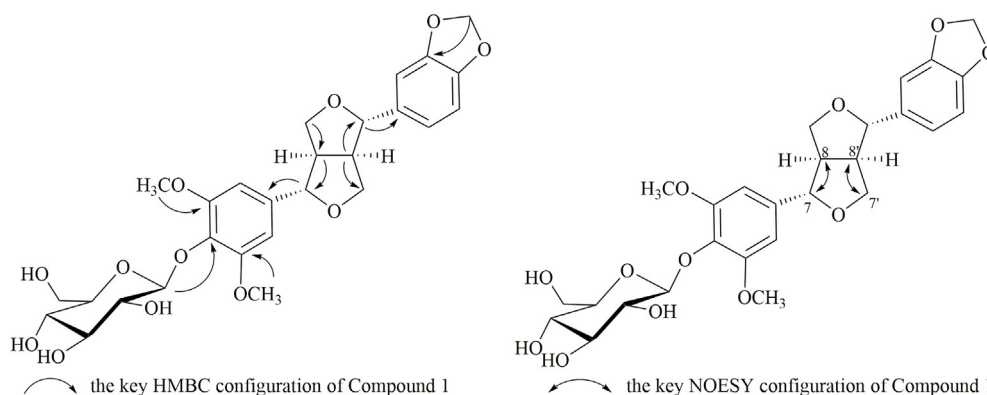


Fig. 2. HMBC and NOESY configuration of compounds 1 (A1).

in section 2.5. Cell supernatant levels of TNF- $\alpha$ , IL-6, IFN- $\gamma$  were measured by CBA mice Inflammation Kit (BD Biosciences, Heidelberg, Germany). 50  $\mu$ l of cell supernatant was incubated with 50  $\mu$ l of *anti*-TNF- $\alpha$  (558299, BD), *anti*-IL-6 (558301, BD), *anti*-IFN- $\gamma$  (558296, BD) antibody (which was conjugated to beads) and 50  $\mu$ l of the PE-labeled *anti*-TNF- $\alpha$ , *anti*-IL-2, *anti*-IFN- $\gamma$  and *anti*-IL-10 in the dark at room temperature for 2 h with sufficient shaking. After washing with CBA wash buffer, the samples were resuspended in 500  $\mu$ l of CBA wash buffer and analyzed immediately using a flow cytometry (FACS Aria III, BD Biosciences, USA) and the Cell Quest software (BD).

## 2.7. Apoptosis assay

H9c2 cells were seeded on 6-well plates ( $5 \times 10^5$  cells/well) and allowed to adhere overnight. Anti-apoptotic effects of compound 1 and compound 2 (10  $\mu$ M) on H9c2 cells were evaluated by Annexin V/PI double staining according to the manufacturer's instructions (BD Biosciences 556547, United States). Briefly, cells were harvested after 24 h treatment (LPS 20  $\mu$ g/mL, compound 10  $\mu$ M), and  $1 \times 10^5$  cells were then incubated in 100  $\mu$ L labeling solution (5  $\mu$ L of Annexin V-FITC, 5  $\mu$ L of PI, 10  $\mu$ L of 10X binding buffer, and 80  $\mu$ L of binding buffer) in darkness at room temperature for 15 min. After that, 400  $\mu$ L of 1X binding buffer was added to stop the staining reaction. Flow cytometric analyses were performed on a FACS AriaIII (BD Biosciences, USA) utilizing 10,000 events. Three independent experiments were performed.

## 2.8. Determination of ROS levels

The production of ROS in the H9C2 cells was fluorometrically monitored using the nonfluorescent probe, 2,7-dichlorofluorescein diacetate (DCFH-DA) (CA1410; Beijing Solarbio Science & Technology Co.,

Ltd, China). Cells in each group cultured on 6-well plates (same as 2.7.) were trypsinized and collected by centrifugation. DCFH-DA (1  $\mu$ M) was added to the H9c2 cells and incubated at 37  $^{\circ}$ C for 20 min. Subsequently, H9c2 cells were washed thrice with PBS, and the DCF fluorescence was measured by flow cytometry [20].

## 2.9. Cellular immunofluorescence

Assay for cellular immunofluorescence was performed in 96-well plates (E190236X, PerkinElmer, USA). After treatment (same as section 2.5.), the cells were fixed with 4% paraformaldehyde for 20 min at room temperature. The cell monolayers were blocked for 90 min and then incubated with primary antibodies (TLR4 ab22048, p-cJUN ab30620, p-P65 ab86299, p-IRF3 SAB4503926, cleaved caspase-3 ab214430) diluted in blocking buffer (1:200, 50  $\mu$ l) overnight at 4  $^{\circ}$ C. After washing with PBS with Tween-20 (PBST) buffer, the cell layers were stained with the anti-mouse IgG or anti-rabbit IgG (1918277 or 1981155, 1:500, 50  $\mu$ l; ThermoFisher Scientific, USA) for 1 h at room temperature, rinsed, and scanned using an High-content imaging system (Opera Phenix, PerkinElmer, USA). The relative protein expression level was normalized against the Harmony 4.8.

## 2.10. Western blot

H9c2 cells were seeded and treated as described in Section 2.9. Cell extracts were prepared, electrophoresed under denaturing conditions. The proteins were transferred onto polyvinylidene difluoride membranes. The membranes were washed in PBST and incubated overnight at 4  $^{\circ}$ C with corresponding primary antibodies (p-P65 ab86299, p-c-JUN ab32385, SAB4503906 Sigma). The membranes were then incubated with secondary antibodies (goat anti-rabbit 925-68071, goat-mouse 925-32210, Li-COR, MO, USA) and the intensity of the proteins was

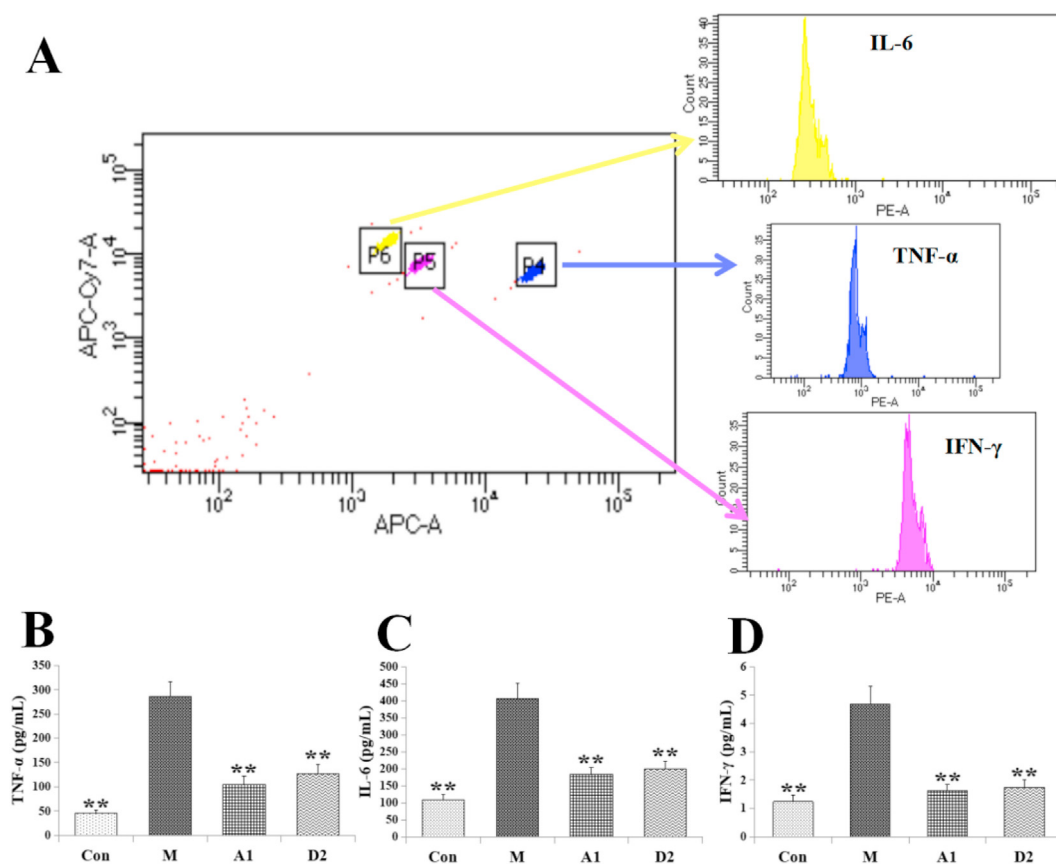


**Fig. 3.** Effects of A1 and D2 on the production of cytokines in LPS-stimulated H9c2 cells using flow cytometry. The cells were incubated with the indicated concentrations of A1 and D2 (10  $\mu$ M) for 1 h and then stimulated with LPS (20  $\mu$ g/mL) for 24 h. Cytokines production was quantified by CBA using flow cytometry. A: Flow diagram. B: TNF- $\alpha$ . C: IL-6. D: IFN- $\gamma$ .  $\bar{x} \pm$  SD,  $n = 4$ , \* $p < 0.05$ , \*\* $p < 0.01$  vs. model group.

quantified using Odyssey (Clx, Li-COR Biosciences, USA).

### 2.11. Molecular docking

The TLR4-MD-2 complex was used as the receptor (PDB: 5LJD), which was downloaded from the ZINC database (ID: ZINC01280591). Since TLR4 needs to bind to the MD-2 protein for the combined TLR4-MD-2 complex to recognize LPS and further induce the activation of the TLR4 protein, the cavity in MD-2 of the TLR4-MD-2 complex was treated as a docking site. Molecular docking was performed using the AutoDock 4.2.6 software.

### 2.12. Statistical analysis

Data were analyzed using SPSS 20.0 (IBM, NY, USA). Statistical significance was assessed in comparison with the respective control for each experiment using one-way analysis of variance (ANOVA). P values less than 0.05 were accepted as significant.

## 3. Results

### 3.1. Identification

Compound **1** was obtained as a pale yellow amorphous powder, with the molecular formula of  $C_{27}H_{32}O_{12}$  deduced from the NMR spectral data and the molecular ion peak at  $m/z = 571.1771$  [ $M + Na$ ] $^+$  (calcd.: 571.1791) in HR-ESI-MS. Compound **1** displayed a similar UV absorption spectrum to that of furofurano ligands at 206 ( $\log \epsilon$  2.42), 228 ( $\log \epsilon$  0.59) and 284 ( $\log \epsilon$  0.23) nm [21]. The IR spectrum showed absorptions for hydroxyl (3445  $cm^{-1}$ ), methoxygroup (2925  $cm^{-1}$ )

and ether groups (1202, 1123 and 1036  $cm^{-1}$ ). The  $^1H$ - and  $^{13}C$  NMR spectra indicated that it was an unsymmetrically substituted furofurano-lignan. The  $^1H$  NMR signals of an ABX system at  $\delta$  6.87 (1H, d,  $J = 2.0$  Hz, H-2'), 6.84 (1H, d,  $J = 8.0$  Hz, H-5') and 6.77 (1H, dd,  $J = 2.0, 8.0$  Hz, H-6'), a 1,3,4,5-substituted aromatic ring at 6.70 (2H, s, H-2, 6), a methylenedioxy group at  $\delta_H$  5.92 (2H, s,  $-OCH_2-$ ), an anomeric proton of the  $\beta$ -glucopyranose moieties resonated at  $\delta_H$  4.80 (1H, d,  $J = 8.0$  Hz, H-1'') and two methoxygroups at  $\delta_H$  3.85 (6H, s,  $2 \times OCH_3$ ). The  $^{13}C$  NMR spectroscopic data of **1** was similar to those of (1R,2S,5R,6R)-5'-O-methylpluviatilol [22], except for the additional signals associated with a glucopyranosyl unit concluded the signals  $\delta_{105.3, 75.7, 78.3, 71.3, 77.8, 62.6}$ . On acid hydrolysis, compound **1** gave D-(+)-glucose, which was identified by HPLC with standard D-(+)-glucose. The cross-peak between H-1'' of glucose and C-4 of the aglycon HMBC spectrum indicated that the glucose unit was connected to C-4 of the compound. The coupling constant between H-7 and H-8 was measured to be 5.0 Hz, which resulted in an erythro configuration at H-7 and H-8. Also, the NOE cross peaks observed between H-7 and H-8 indicated the relative configuration to be *cis*. The relative configuration of H-7' and H-8' was also indicated to be *cis* through the above methods. In addition, the absolute configuration of **1** was defined by CD spectrum. The CD spectrum of **1** showed similar Cotton effects (negative at 199 nm and positive at 212, 239, 278 nm) to that of (1R,2S,5R,6S)-(-)-methylpiperitol [23,24]. Therefore, the asymmetric centers of **1** were 7S,7'S,8R,8'R-configuration. From these data, the structure of **1** was established and named as Dendranlignan A. In addition, the HMBC and NOESY configuration of compounds **1** (A1) were shown in Fig. 2.

The NMR spectroscopic data of compound **2** (Table 1) was similar to that of compound **1**, except for the substitution types of benzene rings.

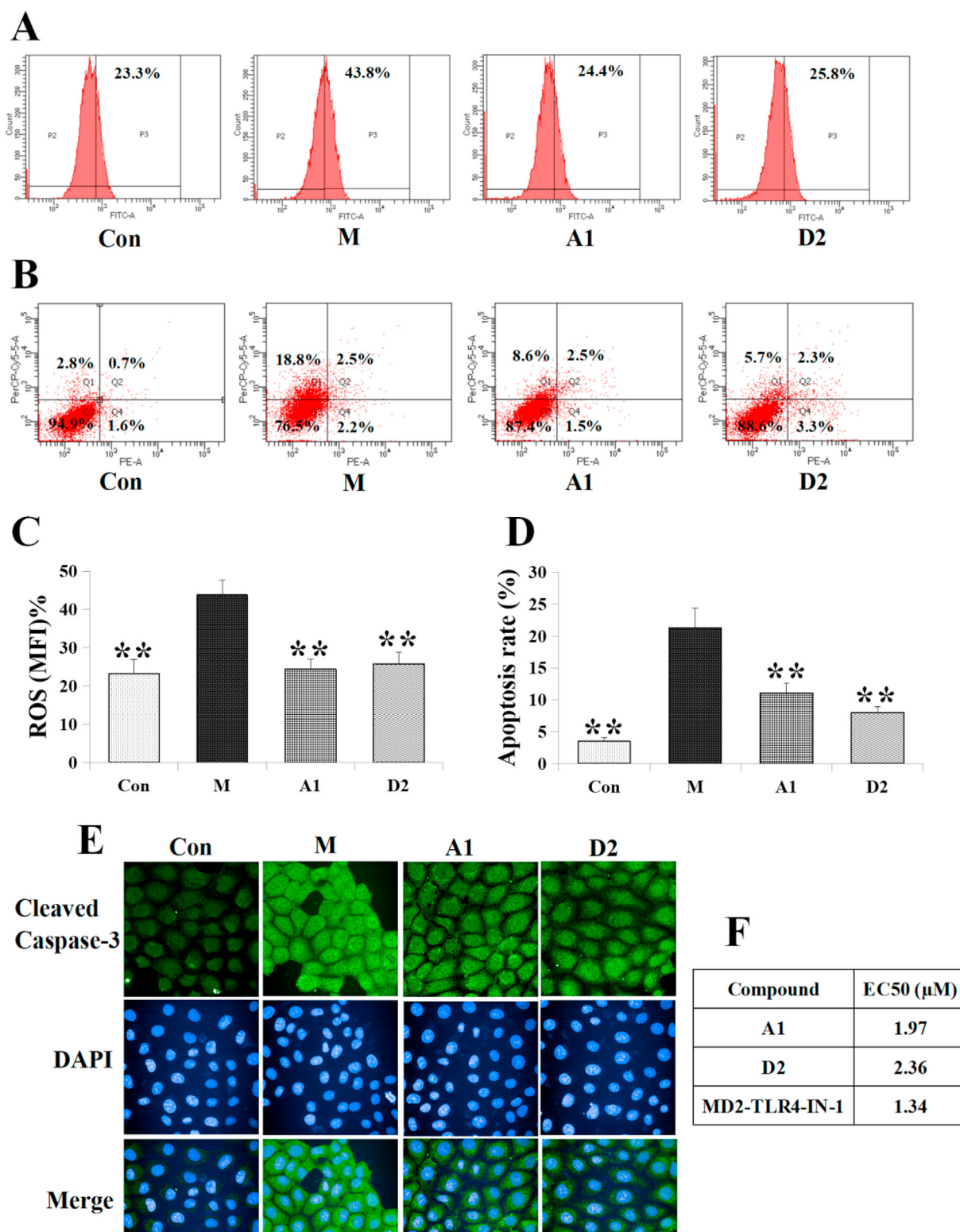


**Fig. 4.** Effects of A1 and D2 on ROS and apoptosis in LPS-induced H9c2 cells using flow cytometry. The cells were incubated with the indicated concentrations of A1 and D2 (10  $\mu\text{M}$ ) for 1 h and then stimulated with LPS (20  $\mu\text{g}/\text{mL}$ ) for 24 h. ROS and apoptosis were quantified by flow cytometry. A: ROS. B: apoptosis. C: Quantization of ROS. D: Quantization of Apoptosis. E: Cleaved caspase-3. F: EC50 of A1 and D2. MD2-TLR4-IN-1, positive control compound, inhibitors for TLR4.  $x \pm \text{SD}$ ,  $n = 4$ , \* $p < 0.05$ , \*\* $p < 0.01$  vs. model group.

The  $^1\text{H}$  NMR data of **2** (Table 1) indicated the presence of two ABX patterns [ $\delta_{\text{H}}$  6.87 (1H, d,  $J = 2.0$  Hz, H-2), 6.77 (1H, d,  $J = 8.0$  Hz, H-5), 6.83 (1H, dd,  $J = 2.0, 8.0$ , H-6) and 7.01 (1H, d,  $J = 2.0$ , H-2'), 7.13 (1H, d,  $J = 8.0$ , H-5'), 6.90 (1H, dd,  $J = 2.0, 8.0$ , H-6')]. According to analyzing the  $^{13}\text{C}$  NMR, HSQC and HMBC spectrum, compound **2** was

determined to lantibeside D compared with the literature [21], and the structure was shown in Fig. 1.

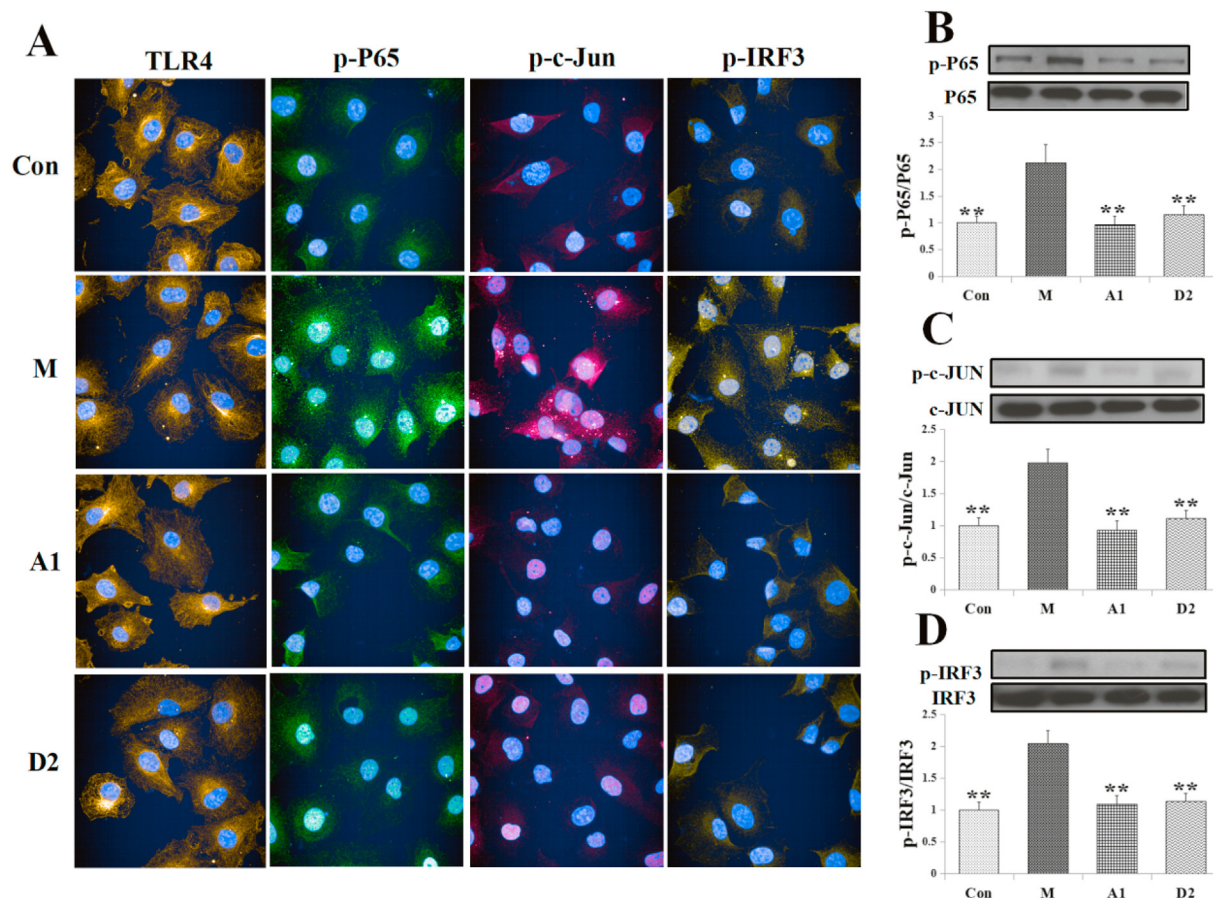


**Fig. 5.** Effects of A1 and D2 on the levels of TLR4, p-cJUN, p-P65, p-IRF3 in LPS-stimulated H9c2 cells. Cells were treated with A1 and D2 at the indicated concentrations (10  $\mu$ M) for 1h and then stimulated with LPS for 60 min. Total and phosphorylated forms of corresponding proteins were detected by cellular immunofluorescence. A: Cell immunofluorescence. B: p-P65/P65. C: p-c-JUN/c-JUN. D: p-IRF3/IRF3.  $x \pm SD$ ,  $n = 4$ ,  $*p < 0.05$ ,  $**p < 0.01$  vs. model group.

### 3.2. A1 and D2 decreased the production of inflammatory cytokines in LPS-induced H9c2 cells

To assess the effect of A1 and D2 on the proinflammatory cytokine production, the levels of TNF- $\alpha$ , IL-6, IFN- $\gamma$  were evaluated by CBA using flow cytometry. As shown in Fig. 3, LPS significantly elevated the levels of inflammatory cytokines TNF $\alpha$ , IL-6, IFN- $\gamma$  while A1 and D2 attenuated LPS-induced changes in the levels of inflammatory cytokines to different degrees in the LPS-induced H9c2 cells.

### 3.3. Effects of A1 and D2 on ROS and apoptosis in LPS-stimulated H9c2 cells

The results of flow cytometry illustrate that the levels of ROS in LPS-induced H9c2 cells was significantly increased, while A1 and D2 pretreatment significantly reduced this increase (Fig. 4A, C). Moreover, flow cytometry analyses show that the rate of LPS-induced H9c2 cell apoptosis was significantly higher than that in the control group ( $p < 0.05$ ). A1 and D2 significantly reduced the apoptosis of LPS-induced H9c2 cells (Fig. 4B, D). In addition, A1 and D2 significantly increased the cell viability of LPS-induced H9c2, results of EC50 indicated that A1 (1.97  $\mu$ M) and D2 (2.36  $\mu$ M) were likely to be inhibitors of TLR4 (Fig. 4F).

### 3.4. Effects of A1 and D2 on the expression of TLR4, p-cJUN, p-P65, p-IRF3 in LPS-induced H9c2 cell

The nuclear protein levels of IRF3, NF- $\kappa$ B heterodimer components (p65) and one of the AP-1 components (c-Jun) was found to be

markedly increased after 1 h of LPS stimulation. A1 and D2 treatment significantly reduced their nuclear localization and the levels of phosphorylated (Fig. 5), suggesting that A1 and D2 inhibits TLR4 signaling. However, we did not observe any significant influence of A1 and D2 on the protein expressions of TLR4 (Fig. 5), MyD88 and TRIF (data not shown).

### 3.5. Interaction between A1, D2 and MD-2 active-site residues

From the molecular docking analysis, it was revealed that the hydrophobic cavity in MD-2 that recognized LPS was large enough to occupy A1 or D2, and formed strong hydrophobic interactions with the ligand binding site (A1: LEU78, ARG90, GLU437, ARG434, SER413. D2: GLU92, ARG90, PHE126, PHE438, SER413, ARG434). After stable binding in the cavity, A1 and D2 occupied the LPS binding site of TLR4-MD-2 (Fig. 6).

## 4. Discussion

*Dendranthema morifolium* (Ramat.) (Flos chrysanthemum) is a commonly used traditional Chinese herb medicinal for treating inflammatory disorders such as acute lung injury [25] and colitis [26]. Although, the literature shows that Huai Flos chrysanthemum has its use in various inflammatory conditions, there is still a lack of research on the anti-inflammatory effect and its mechanism of action. Our laboratory has been engaged in the research on the chemical components and pharmacological effects. In our earlier report, it has been clear that 8 compounds isolated from Huai Flos chrysanthemum have protective effects on LPS-induced cardiomyocytes. Based on the previous research,



## MD-2.

In conclusion, we for the first time discovered a new bisepoxyignan compound A1, and found that this compound has a potential to inhibit inflammation by inhibiting TLR4 signaling.

#### Authorship contribution statement

Mengnan Zeng, Xiaoke Zheng and Meng Li designed and performed the experiments and analyzed the raw data. Yangang Cao, Yingjie Chen, Jingke Zhang, Beibei Zhang assisted with the experiments. Zhiling Yu and Weisheng Feng supervised the project.

#### Declaration of competing interest

The authors declare that they have no known competing financial interests or personal relationships that could have appeared to influence the work reported in this paper.

#### Acknowledgments

This study was supported by the National Key Research and Development Project (2019YFC1708802, 2017YFC1702800) and Henan province high-level personnel special support “ZhongYuan One Thousand People Plan” -Zhongyuan Leading Talent (ZYQR201810080) and the Central Government Guide Local Science and Technology Development Funds ([2016]149).

#### References

- [1] J.D. Sammon, D.E. Klett, A. Sood, et al., Sepsis after major cancer surgery, *J. Surg. Res.* 193 (2015) 788–794.
- [2] M. Merx, C. Weber, Sepsis and the heart, *Circulation* 116 (2007) 793–802.
- [3] P. Yang, Y. Han, L. Gui, et al., Gastrodin attenuation of the inflammatory response in H9C2 cardiomyocytes involves inhibition of NF- $\kappa$ B and MAPKs activation via the phos-phatidylinositol 3-kinase signaling, *Biochem. Pharmacol.* 85 (2013) 1124–1133.
- [4] M. Maeder, T. Fehr, H. Rickli, et al., Sepsis-associated myocardial dysfunction--diagnostic and prognostic impact of cardiac troponins and natriuretic peptides, *Chest* 129 (2006) 1349–1366.
- [5] S.L. Zanotti, S.M. Hollenberg, Cardiac dysfunction in severe sepsis and septic shock, *Curr. Opin. Crit. Care* 15 (2009) 392–397.
- [6] A. Ayala, M. Perl, F. Venet, et al., Apoptosis in sepsis:mechanisms,clinical impact and potential therapeutic targets, *Curr. Pharmaceut. Des.* 14 (2008) 1853–1859.
- [7] H. Zhou, Y. Yuan, Y. Liu, et al., Icaritin protects H9c2 cardiomyocytes from lipopolysaccharide-induced injury via inhibition of the reactive oxygen species-dependent c-Jun N-terminal kinases/nuclear factor - kappa B pathway, *Mol. Med. Rep.* 11 (2015) 4327–4332.
- [8] Y. He, Z. Du, H. Lv, Q. Jia, Z. Tang, et al., Green synthesis of silver nanoparticles by *Chrysanthemum morifolium* Ramat. Extract and their application in clinical ultrasound gel, *Int. J. Nanomed.* 8 (2013) 1809–1815.
- [9] G.H. Lin, L. Lin, H.W. Liang, X. Ma, et al., Antioxidant action of a *Chrysanthemum morifolium* extract protects rat brain against ischemia and reperfusion injury, *Med. Food* 13 (2010) 306–311.
- [10] C.K. Lii, Y.P. Lei, H.T. Yao, Y.S. Hsieh, et al., *Chrysanthemum morifolium* Ramat. reduces the oxidized LDL-induced expression of intercellular adhesion molecule-1 and E-selectin in human umbilical vein endothelial cells, *Ethnopharmacol* 128 (2010) 213–220.
- [11] J. Yuan, J. Huang, G. Wu, et al., Multiple responses optimization of ultrasonic-assisted extraction by response surface methodology (RSM) for rapid analysis of bioactive compounds in the flower head of *Chrysanthemum morifolium* Ramat, *Ind. Crop. Prod.* 74 (2015) (2015) 192–199.
- [12] L. Qu, J.Y. Ruan, L.Y. Jin, et al., Xanthine oxidase inhibitory effects of the constituents of *Chrysanthemum morifolium* stems, *Phytochem. Lett.* 19 (2017) 39–45.
- [13] Chinese Pharmacopoeia Committee, “Pharmacopoeia of the People's Republic of China,” Part 1, China Medical Science Press, Beijing, 2015, pp. 310–311.
- [14] W.J. Chen, M.N. Zeng, M. Li, et al., Four new sesquiterpenoids from *Dendranthema morifolium* (Ramat.) kitam flowers, *Phytochem. Lett.* 23 (2018) 52–56.
- [15] B.B. Zhang, M.N. Zeng, M. Li, et al., Guaiane-type sesquiterpenoids from *Dendranthema morifolium* (Ramat.) S. Kitam flowers protect H9c2 cardiomyocyte from LPS-induced injury, *Nat. Prod. Commun.* 14 (2019), <https://doi.org/10.1177/1934578X19864179>.
- [16] Y. Alhamdi, S.T. Abrams, Z. Cheng, et al., Circulating histones are major mediators of cardiac injury in patients with sepsis, *Crit. Care Med.* 43 (2015) 2094–2103.
- [17] P.C. Trivedi, J.J. Bartlett, L.J. Perez, et al., Glucolipototoxicity diminishes cardiomyocyte TFEB and inhibits lysosomal autophagy during obesity and diabetes, *Biochim. Biophys. Acta* 1861 (2016) 1893–1910.
- [18] A.N. Velic, D. Laturmus, J. Chhoun, et al., Diabetic basement membrane thickening does not occur in myocardial capillaries of transgenic mice when metallothionein is overexpressed in cardiac myocytes, *Anat. Rec.* 296 (2013) 480–487.
- [19] Y.G. Cao, Y.L. Zhang, M.N. Zeng, et al., Renoprotective mono- and triterpenoids from the fruit of *Gardenia jasminoides*, *J. Nat. Prod.* 83 (2020) 1118–1130.
- [20] M.N. Zeng, M. Qi, Y. Wang, et al., 5-O-methylidihydroquercetin and cilicicone B isolated from *Spina Gleditsiae* ameliorate lipopolysaccharide-induced acute kidney injury in mice by inhibiting inflammation and oxidative stress via the TLR4/MyD88/TRIF/NLRP3 signaling pathway, *Int. Immunopharm.* 80 (2020) 106194.
- [21] T. Li, X.J. Hao, Q.Q. Gu, W.M. Zhu, Minor furofuran lignans from the Tibetan herb, *Lancea tibetica*, *Planta Med.* 74 (2008) 1391–1396.
- [22] T.H. Quang, N.T. Ngan, C.V. Minh, P.V. Kiem, et al., Anti-inflammatory and PPAR transactivational effects of secondary metabolites from the roots of *Asarum sieboldii*, *Bioorg. Med. Chem. Lett.* 22 (2012) 2527–2533.
- [23] H. Wu, Z. Li, Q. Zhang, Y. Pei, Application of CD in study of the absolute configuration of lignans, *J. Shenyang Pharm. Univ.* 27 (2010) 587–594.
- [24] O. Hofer, R. Schoim, Stereochemistry of tetrahydrofuran derivatives-circular dichroism and absolute conformation, *Tetrahedron* 37 (1981) 1181–1186.
- [25] X.H. Zhang, Study on the Changes of Chemical Composition, Anti-inflammatory Efficacy and Mechanism of Different Cultivars of *Fios Chrysanthemi*, Nanjing University of Chinese Medicine, Nanjing, 2014.
- [26] J.H. Tao, J.A. Duan, W. Zhang, et al., Polysaccharides from *Chrysanthemum morifolium* Ramat ameliorate colitis rats via regulation of the metabolic profiling and NF- $\kappa$ B/TLR4 and IL-6/JAK2/STAT3 signaling pathways, *Front. Pharmacol.* 9 (2018) 746.
- [27] Y.E. Wang, A.M. Abarbanell, J.L. Herrmann, et al., Toll-like receptor signaling pathways and the evidence linking toll-like receptor signaling to cardiac ischemia/reperfusion injury, *Shock* 34 (2010) 548–557.
- [28] X. Cheng, Y.L. Yang, H. Yang, et al., Kaempferol alleviates LPS-induced neuroinflammation and BBB dysfunction in mice via inhibiting HMGB1 release and down-regulating TLR4/Myd88 pathway, *Int. Immunopharm.* 56 (2018) 29–35.
- [29] N.J. Gay, M.F. Symmons, M.A. Gangloff, Assembly and localization of Toll-like receptor signalling complexes, *Nat. Rev. Immunol.* 14 (2014) 546–558.
- [30] M. Sasai, M. Tatematsu, H. Oshiumi, et al., Direct binding of TRAF2 and TRAF6 to TICAM-1/TRIF adaptor participates in activation of the Toll-like receptor3/4 pathway, *Mol. Immunol.* 47 (2010) 1283–1291.